

# Geophysical Research Letters



## RESEARCH LETTER

10.1029/2018GL081731

### Key Points:

- Long-term measurements show no large increases in U.S. methane emissions in the past decade
- The estimated increase in U.S. oil and natural gas CH<sub>4</sub> emissions is an order of magnitude lower than some previous studies
- The increasing trend in C<sub>2</sub>H<sub>6</sub>/CH<sub>4</sub> emission ratios has resulted in major overestimation of an oil and gas emissions trend in some previous studies

### Supporting Information:

- Supporting Information S1

### Correspondence to:

X. Lan,  
xin.lan@noaa.gov

### Citation:

Lan, X., Tans, P., Sweeney, C., Andrews, A., Dlugokencky, E., Schwietzke, S., et al. (2019). Long-term measurements show little evidence for large increases in total U.S. methane emissions over the past decade. *Geophysical Research Letters*, 46, 4991–4999. <https://doi.org/10.1029/2018GL081731>

Received 17 DEC 2018

Accepted 18 APR 2019

Accepted article online 25 APR 2019

Published online 15 MAY 2019

## Long-Term Measurements Show Little Evidence for Large Increases in Total U.S. Methane Emissions Over the Past Decade

Xin Lan<sup>1,2</sup> , Pieter Tans<sup>2</sup> , Colm Sweeney<sup>2</sup> , Arlyn Andrews<sup>2</sup> , Edward Dlugokencky<sup>2</sup> , Stefan Schwietzke<sup>1,2</sup> , Jonathan Kofler<sup>1,2</sup> , Kathryn McKain<sup>1,2</sup> , Kirk Thoning<sup>2</sup> , Molly Croftwell<sup>1,2</sup> , Stephen Montzka<sup>2</sup> , Benjamin R. Miller<sup>1,2</sup> , and Sébastien C. Biraud<sup>3</sup>

<sup>1</sup>Cooperative Institute for Research in Environmental Sciences, University of Colorado Boulder, Boulder, CO, USA,

<sup>2</sup>National Oceanic and Atmospheric Administration, Earth System Research Laboratory, Boulder, CO, USA, <sup>3</sup>Lawrence Berkeley National Laboratory, Berkeley, CA, USA

**Abstract** Recent studies show conflicting estimates of trends in methane (CH<sub>4</sub>) emissions from oil and natural gas (ONG) operations in the United States. We analyze atmospheric CH<sub>4</sub> measurements from 20 North American sites in the National Oceanic and Atmospheric Administration Global Greenhouse Gas Reference Network and determined trends for 2006–2015. Using CH<sub>4</sub> vertical gradients as an indicator of regional surface emissions, we find no significant increase in emissions at most sites and modest increases at three sites heavily influenced by ONG activities. Our estimated increases in North American ONG CH<sub>4</sub> emissions (on average approximately  $3.4 \pm 1.4$  %/year for 2006–2015,  $\pm\sigma$ ) are much smaller than estimates from some previous studies and below our detection threshold for total emissions increases at the east coast sites that are sensitive to U.S. outflows. We also find an increasing trend in ethane/methane emission ratios, which has resulted in major overestimation of oil and gas emissions trends in some previous studies.

**Plain Language Summary** In the past decade, natural gas production in the United States has increased by ~46%. Methane emissions associated with oil and natural gas productions have raised concerns since methane is a potent greenhouse gas with the second largest influence on global warming. Recent studies show conflicting results regarding whether methane emissions from oil and gas operations have been increased in the United States. Based on long-term and well-calibrated measurements, we find that (i) there is no large increase of total methane emissions in the United States in the past decade; (ii) there is a modest increase in oil and gas methane emissions, but this increase is much lower than some previous studies suggest; and (iii) the assumption of a time-constant relationship between methane and ethane emissions has resulted in major overestimation of an oil and gas emissions trend in some previous studies.

## 1. Introduction

Atmospheric CH<sub>4</sub> is a well-mixed greenhouse gas with the second largest increase in radiative forcing after carbon dioxide (Butler & Montzka, 2017). It can be released from natural (e.g., wetlands, wild animals, and termites) and anthropogenic sources (e.g., oil and natural gas [ONG] operations, landfills, and agriculture; United States Environmental Protection Agency [EPA], 2017, Saunio et al., 2016). The global atmospheric CH<sub>4</sub> abundance was nearly stable from 1999 through 2006 (Bousquet et al., 2006; Dlugokencky et al., 2003; Dlugokencky et al., 2009), but since then has significantly increased (Dlugokencky, 2018; Nisbet et al., 2016). ONG activities are a large source of atmospheric CH<sub>4</sub> and alkanes such as ethane (C<sub>2</sub>H<sub>6</sub>), propane (C<sub>3</sub>H<sub>8</sub>), and others. In the past decade, natural gas production has increased by ~46% in the United States (Figure S1 in the supporting information) due to the development of horizontal drilling and hydraulic-fracturing techniques (U.S. Energy Information Administration, 2016). Several studies conclude that there are substantial increases in ONG CH<sub>4</sub> emissions (Franco et al., 2016; Hausmann et al., 2016; Helmig et al., 2016; Turner et al., 2016), with some (Hausmann et al., 2016; Turner et al., 2016) further suggesting that these have substantially contributed to the global CH<sub>4</sub> increases after 2007. Ethane/methane emission ratios have been used to argue for large increases in ONG CH<sub>4</sub> emissions (Franco et al., 2016; Hausmann et al., 2016; Helmig et al., 2016), since C<sub>2</sub>H<sub>6</sub> and CH<sub>4</sub> are coemitted from ONG activities, although Helmig et al. (2016) notes an inconsistency with measurements of CH<sub>4</sub> and its isotopic ratios ( $\delta^{13}\text{CH}_4$ ). Measured changes of  $\delta^{13}\text{CH}_4$  lead to the hypothesis that the global CH<sub>4</sub> rise after 2007 is dominated by biogenic

©2019. The Authors.

This is an open access article under the terms of the Creative Commons Attribution-NonCommercial-NoDerivs License, which permits use and distribution in any medium, provided the original work is properly cited, the use is non-commercial and no modifications or adaptations are made.

emissions (Nisbet et al., 2016; Schaefer et al., 2016; Schwietzke et al., 2016). A recent study using an ensemble of global atmospheric inversions constrained by surface observations, with some including satellite retrievals of column-averaged CH<sub>4</sub>, finds no statistically significant increase in total North American CH<sub>4</sub> emissions during 2000–2014 (Bruhwiler et al., 2017).

Here we analyze decadal records of CH<sub>4</sub> (2006–2015) and C<sub>3</sub>H<sub>8</sub> (2008–2015) from 11 sites where CH<sub>4</sub> vertical profiles are collected from aircraft (Sweeney et al., 2015) and 9 surface sites (including tall towers; Andrews et al., 2014) in the National Oceanic and Atmospheric Administration Global Greenhouse Gas Reference Network (GGGRN; see Figure S2 for site locations). The majority of the sites are designed to capture air masses that are well mixed and thus represent influences of emissions from large areas. According to our footprint and inventory (Maasackers et al., 2016) analysis in which the sensitivity of observed mole fraction changes to emissions from different sources are estimated (see Figure S3 for footprints), five GGGRN sites are substantially influenced by ONG activities (DND, CAR, SGP, SGP-s, and WKT-s; ‘-s’ following a site code indicates surface site; site codes are given in Table S1 in the supporting information). Thus, these five sites are defined as ‘ONG sites’ in the following text. The other sites are defined as ‘non-ONG sites’, although some of them are moderately influenced by ONG emissions. Please refer to Supporting Information (SI) for details of measurement and statistical analysis.

## 2. Trends in CH<sub>4</sub> and CH<sub>4</sub> Vertical Gradients ( $\Delta$ CH<sub>4</sub>)

Atmospheric methane trends from GGGRN sites demonstrate clear increases after 2006 (e.g., Figures 1a and 1b), similar to the global background CH<sub>4</sub> trend. Excluding the five ONG sites, CH<sub>4</sub> trends in the United States (contiguous 48 states, ‘CONUS’) are indistinguishable within 1 $\sigma$  uncertainty with an average increase rate of  $6.12 \pm 0.11$  ppb/year ( $0.33 \pm 0.01\%$ /year). This is similar to the trends in the marine boundary layer reference (Dlugokency et al., 2015) of  $6.11 \pm 0.07$  ppb/year for the 25–55°N zonal average and of  $6.08 \pm 0.04$  ppb/year for the global average. For the five ONG sites, a significantly larger trend is measured in CH<sub>4</sub> mole fractions, which is  $7.65 \pm 0.31$  ppb/year ( $0.40 \pm 0.02\%$ /year).

To reveal trends in CONUS CH<sub>4</sub> emissions, we assess CH<sub>4</sub> mole fraction enhancements ( $\Delta$ ) after removing appropriate background mole fractions, because the background contributes the largest part of CH<sub>4</sub> in ambient air, while enhancements due to regional and local emissions are relatively small. A trend in CH<sub>4</sub> mole fractions (see above) without subtracting the background signals cannot represent the trend in local and regional emissions. We use the midtroposphere (3.5–5.5 km above sea level) as representative of background condition and investigate the trends in  $\Delta$ CH<sub>4</sub>, which are, in this case, also vertical gradients (e.g., Figures 1c and 1d; see SI section 3 for calculation). A lower boundary of 3.5 km ensures free troposphere air, and the upper boundary ensures that the background air masses are not completely detached from the surface since measurements of CH<sub>4</sub> and its trend at high altitudes may considerably lag surface CH<sub>4</sub> in time and be influenced by the stratosphere. Free troposphere measurements have been used as background references in previous studies of CO<sub>2</sub> (including its isotopic ratios), which also has a large background signal (Ballantyne et al., 2010; Miller et al., 2012). We do not use west coast sites as background reference for all CONUS sites since a large fraction of the air masses we measure are not from the western sector directly (see Figure S2 for average wind pattern). The vertical gradient of CH<sub>4</sub> has been proposed as a more sensitive indicator of surface emissions than horizontal gradients (Bruhwiler et al., 2017). When CH<sub>4</sub> is emitted at the surface, the enhanced CH<sub>4</sub> is mostly retained within the planetary boundary layer (typically below 2.5 km above sea level) for several days, while the free troposphere receives a considerably smaller local influence and mostly represents well-mixed background air (Sweeney et al., 2015). East coast sites that are downwind of CONUS emissions show much larger vertical gradients (39.3 ppb for the average of the NHA and SCA sites; see Table S2) than the west coast inflow site (12.0 ppb at ESP).

We expect to detect trends in vertical gradients if there are increases in surface emissions from locations upwind of a measurement site and no significant change in transport patterns. Our footprint analysis finds that all of the GGGRN sites have similar patterns of surface influences during the first and second halves of the past decade (Figure S4). However, we find no significant trends, meaning the estimated trend is less than 1 $\sigma$  uncertainty of the trend, in the CH<sub>4</sub> vertical gradients ( $\Delta$ CH<sub>4</sub>) at most non-ONG sites (Figures 2 and S6). The average trend in  $\Delta$ CH<sub>4</sub> is  $-0.21 \pm 0.10$  ppb/year ( $-1.00 \pm 0.36\%$ /year) for non-ONG sites. For the five ONG sites, the average trend is  $1.14 \pm 0.30$  ppb/year ( $2.05 \pm 0.58\%$ /year). The average trend for

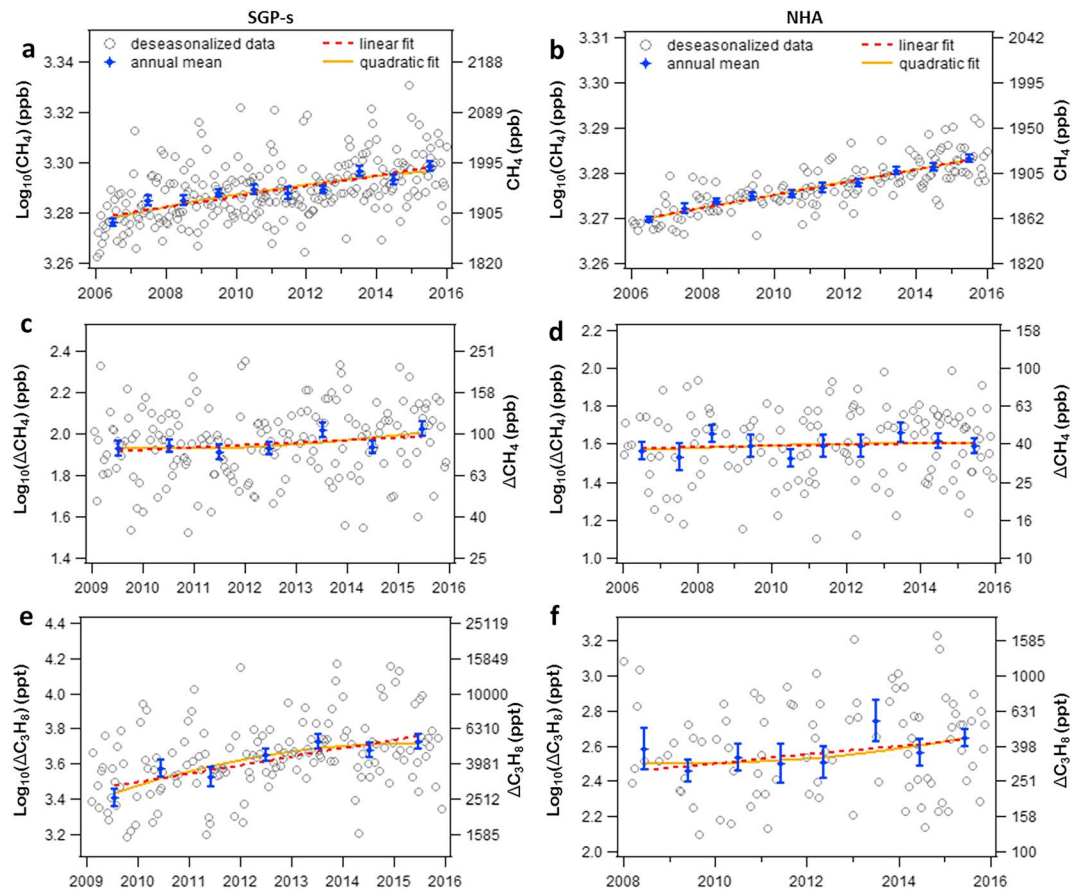


**Figure 1.** Methane and propane data and trend fits. Left column shows data from Southern Great Plains, Oklahoma (SGP-s, an ONG site), and right column shows data from Worcester, Massachusetts (NHA, an east coast outflow site; see Figure S2 for average wind pattern). (a and b) Deseasonalized data and trend fits to those data. For the aircraft site (NHA), those data are the averages below 2.5 km above sea level. (c and d)  $\text{CH}_4$  vertical gradients ( $\Delta\text{CH}_4$ ) and trend fits to those data. (e and f)  $\text{C}_3\text{H}_8$  vertical gradients ( $\Delta\text{C}_3\text{H}_8$ ) and trend fits to those data. Trend fits are performed to annual means and are weighted by the standard errors of the mean (blue error bars; SI section 2). The left axes are in  $\log_{10}$  scale (see SI section 2 for details); labels on the right axes show corresponding values of the ticks on the left axes. Trends are presented in Figures 2 and S6.

east coast sites is  $-0.12 \pm 0.16$  ppb/year ( $-0.10 \pm 0.50\%$ /year). Note that trends in  $\Delta\text{CH}_4$  are contributed by both anthropogenic and natural sources. However, we find strong correlations between  $\Delta\text{CH}_4$  and  $\Delta\text{C}_3\text{H}_8$  (a tracer for ONG emissions) in winter even for non-ONG sites (Figure S5), which is likely due to the reduction in natural  $\text{CH}_4$  emissions during wintertime. Despite the increased wintertime correlation between  $\Delta\text{CH}_4$  and  $\Delta\text{C}_3\text{H}_8$  and the steeper vertical gradients due to the reduced vertical transport, there is no evidence of an increased trend in  $\Delta\text{CH}_4$  during winter (Figure S7) as would be expected if there were significant increases in ONG  $\text{CH}_4$  emissions.

The GGGRN sites are sensitive to ONG emissions because their footprint areas include major ONG production basins in CONUS (Figure S3). However, we find moderate increases in  $\Delta\text{CH}_4$  from three out of five ONG sites (DND, SGP-s, and WKT-s). If we use the ONG trends from these three sites to represent the ONG emissions trend in the United States (see SI section 5 for calculation), the average (weighted by upwind ONG  $\text{CH}_4$  emissions) annual growth rate would be  $3.4 \pm 1.4\%$ /year or  $0.3 \pm 0.1$  Tg/year<sup>2</sup> as a long-term average (note that the relative trend in %/year is independent of inventory estimates of emissions). This estimate is about an order of magnitude lower than estimates from several previous studies showing 2.1–4.4 Tg/year<sup>2</sup> increase (Turner et al., 2016, Franco et al., 2016, Hausmann et al., 2016, Helmig et al., 2016; note different but overlapping study periods). Nevertheless, a few studies suggest an underestimate in the magnitude of  $\text{CH}_4$  emissions in inventories (e.g., Alvarez et al., 2018; Brandt et al., 2014; Miller et al., 2013); our study does not address the magnitude of emissions but only focuses on the trend in emissions that can be estimated

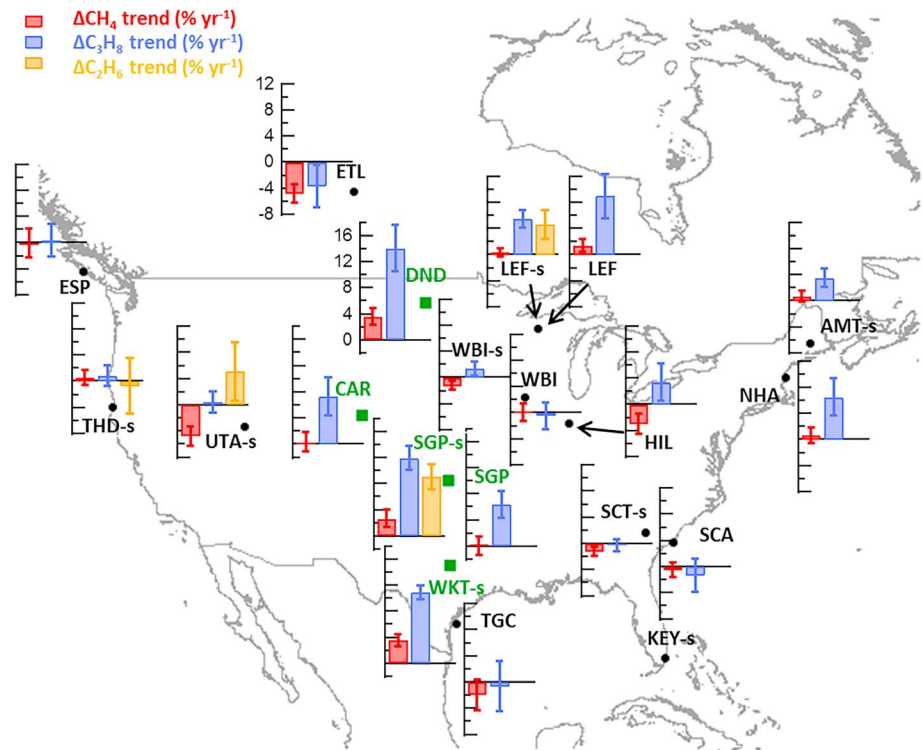


**Figure 2.** Trends in  $\text{CH}_4$ ,  $\text{C}_3\text{H}_8$ , and  $\text{C}_2\text{H}_6$  enhancements ( $\Delta$ ) over North America in recent years (2006–2015 for  $\text{CH}_4$  and 2008–2015 for  $\text{C}_2\text{H}_6$  and  $\text{C}_3\text{H}_8$  for most sites; see Table S1.). The green squares and black dots show ONG and non-ONG sites, respectively. ‘-s’ following a site code indicates surface site. For all bar charts each tick increment is 2%/year and the horizontal axis crosses at 0%/year (e.g., ETL and DND); ‘%/year’ means increase of  $\Delta$  relative to previous year; see Table S2 for values, and trends in ppb/year for  $\text{CH}_4$  or in ppt/year for  $\text{C}_2\text{H}_6$  and  $\text{C}_3\text{H}_8$ . The error bars show  $1\sigma$  uncertainty. For  $\text{CH}_4$  and  $\text{C}_3\text{H}_8$ , enhancements are relative to midtroposphere measurements (thus, the trends are for vertical gradients, also see Figure S6). For  $\text{C}_2\text{H}_6$ , enhancements are relative to the Marine Boundary Layer background (SI section 3).

directly from atmospheric observations. This relatively small trend in ONG emissions ( $3.4 \pm 1.4\%$ /year) is challenging for the east coast sites to detect.

How much do  $\text{CH}_4$  emissions need to increase to be detected by the GGGRN? Since the relative trend in vertical gradients is equal to the relative trend in total regional emissions (both as %/year changes) considering no significant secular changes in atmospheric transport/mixing (as shown in Figure S4), the uncertainty of the trend in vertical gradients can serve as an indicator for the detectability of the trend in emissions. Note that the variability in midtroposphere background has been accounted for in estimating the trend uncertainty (SI section 3). We find that more than half of the sites have trend uncertainties ( $1\sigma$ ) smaller than 1.3%/year (Table S2), which suggests at least half of GGGRN sites can likely detect a relative change of total  $\text{CH}_4$  emissions greater than 1.3%/year (averaged over the 10-year period). The detectability thresholds across four east coast sites (NHA, SCA, SCT-s, and AMT-s) range from 0.7 to 1.2 %/year. Our estimated ONG emission trend of  $3.4 \pm 1.4\%$ /year corresponds to a  $0.7 \pm 0.3\%$ /year increase in total U.S. emissions assuming that ONG emissions account for 20% of total emissions (United States EPA, 2017, Saunio et al., 2016). Thus, these east coast sites are not sensitive enough to clearly capture the relatively small ONG emissions trend (meaning  $0.7 \pm 0.3\%$ /year is not significantly higher than detectability thresholds for east coast sites). Increasing the numbers of vertical profiles and sampling sites would help to decrease uncertainty in trends and better monitor changes in ONG emissions. However, if the large trends of ONG emissions proposed by previous studies exist (Franco et al., 2016; Hausmann et al., 2016; Helmig et al., 2016; Turner et al., 2016), which correspond to trends in total  $\text{CH}_4$  emissions of 5.2–11.0%/year, the east coast sites are capable of detecting them. Such large trends are not apparent in our measurement data from east coast sites making the suggested large increases in U.S. ONG emissions highly unlikely. Note that our trend and detectability are directly calculated from long-term observations, and influences of temporal coverage are fully

considered during calculations (SI section 3). Thus, they are more definitive than model results (Bruhwiler et al., 2017) that are subject to transport and other errors.

In principle, a significant decrease in agricultural CH<sub>4</sub> emissions (mainly from livestock) could have cancelled the increases in ONG emissions given that both emissions are of similar magnitude (United States EPA, 2017). The footprint regions of two ONG sites (SGP-s and WKT-s) overlap with important cattle production regions. To evaluate the potential impact of a livestock emission trend on estimated ONG trends, we impose an agriculture emission trend (-1.7%/year for 2006-2013; Wolf et al., 2017) in calculating the new ONG trends for these two ONG sites (SI section 5). The new ONG trends are  $3.2 \pm 1.3\%$ /year and  $4.8 \pm 1.0\%$ /year for SGP-s and WKT-s, respectively, which are within the uncertainty ranges of our previous estimates. This is expected because both sites are dominated by ONG emissions and non-ONG emissions account for less than 15% of the CH<sub>4</sub> enhancements (Wolf et al., 2017).

We have looked into the influences of non-ONG emissions from measurements at sites that are further away from major ONG production fields, for example, the Great Lakes region. Measurement sites (LEF, LEF-s, WBI, WBI-s, and HIL) in this region have less than 50% ONG influence according to our footprint and inventory analysis. In the warm months, we find increments of  $\Delta\text{CH}_4$  without increments of  $\Delta\text{C}_3\text{H}_8$  (see Figure S5a for LEF site), indicating possible influences from non-ONG CH<sub>4</sub> emissions and/or increased C<sub>3</sub>H<sub>8</sub> losses from faster reactions with hydroxyl radical under higher temperature. Livestock CH<sub>4</sub> emissions from inventories show hot spots in the Great Lake region (Hristov et al., 2017; Maasackers et al., 2016). In addition, the Great Lake region is also downwind of major wetlands (Lehner & Doll, 2004). Thus, the Great Lakes sites should be sensitive to livestock and wetland CH<sub>4</sub> emissions. The mean trend of  $\Delta\text{CH}_4$  in these sites is -0.5%/year. Given the estimated trend detectability of 0.5%/year (estimated using  $\sqrt{\sum_1^5 (\frac{a_i}{5})^2}$ ; deseasonalized data from each site are independent due to different sampling times and frequencies), increases in total emissions in the Great Lakes region are highly unlikely. Even though these sites are influenced by ONG emissions in winter judging from the strong correlation between  $\Delta\text{C}_3\text{H}_8$  and  $\Delta\text{CH}_4$  (Figure S5b), we do not find statistically significant CH<sub>4</sub> trends in winter (Figure S7). Since there are no significant changes in total emissions or ONG emissions in the Great Lakes region, it then implies no significant changes in non-ONG CH<sub>4</sub> emissions in this region in the past decade.

### 3. Discrepancies Between Trends in $\Delta\text{C}_2\text{H}_6$ and $\Delta\text{C}_3\text{H}_8$ and Trends in $\Delta\text{CH}_4$

Our study also finds much larger relative trends (in %/year) in C<sub>2</sub>H<sub>6</sub> and C<sub>3</sub>H<sub>8</sub> enhancements (i.e.,  $\Delta\text{C}_2\text{H}_6$  and  $\Delta\text{C}_3\text{H}_8$ ) than in  $\Delta\text{CH}_4$ ; even at ONG sites that  $\Delta\text{CH}_4$  signals are mostly contributed by ONG activities only (Figure 2). Both C<sub>2</sub>H<sub>6</sub> and C<sub>3</sub>H<sub>8</sub> are coemitted with CH<sub>4</sub> from most ONG sources, and they have much smaller background values than CH<sub>4</sub> (due to shorter atmospheric lifetimes (Goldstein et al., 1995, Rudolph, 1995) and lower emissions), which make them good tracers for ONG emissions. Much larger relative trends (in %/year) in C<sub>3</sub>H<sub>8</sub> vertical gradients ( $\Delta\text{C}_3\text{H}_8$ ) than in  $\Delta\text{CH}_4$  are consistently observed at ONG sites (Figure 2). This suggests larger percentage increases in C<sub>3</sub>H<sub>8</sub> emission than in CH<sub>4</sub> emission from the upwind regions of the sites. For the five ONG sites, the average trend in  $\Delta\text{C}_3\text{H}_8$  is  $10.12 \pm 1.09\%$ /year (see Table S2 for trends in ppt/year); for non-ONG sites, the average trend is  $1.74 \pm 0.64\%$ /year. Long-term records of C<sub>2</sub>H<sub>6</sub> are only available at a few CONUS surface sites. For C<sub>2</sub>H<sub>6</sub> enhancements ( $\Delta\text{C}_2\text{H}_6$ ), the trend at SGP-s (an ONG site) is the largest,  $6.95 \pm 1.28\%$ /year.

### 4. Discrepancies Between Observed and Calculated $\Delta\text{CH}_4$ Trends Using $\Delta\text{C}_2\text{H}_6$ or $\Delta\text{C}_3\text{H}_8$

Strong linear correlations between CH<sub>4</sub> and C<sub>2</sub>H<sub>6</sub> enhancements ( $\Delta\text{CH}_4$  and  $\Delta\text{C}_2\text{H}_6$ ) have been reported from previous ONG field studies with spatially different enhancement ratios (ERs; Peischl et al., 2015, 2016, Smith et al., 2015, Helmig et al., 2014). These ERs may be representative of relative emission rates at the time of the measurement but have been used to estimate trends in ONG CH<sub>4</sub> emissions over longer periods (Franco et al., 2016; Hausmann et al., 2016; Helmig et al., 2016). In contrast, our study determines CH<sub>4</sub> trends in emissions directly from CH<sub>4</sub> observations, and we find much smaller increases in CH<sub>4</sub> ONG emissions than those studies. To investigate this discrepancy, we compared the observed trends of  $\Delta\text{CH}_4$  with  $\Delta\text{CH}_4$  trends estimated using  $\Delta\text{C}_2\text{H}_6$  or  $\Delta\text{C}_3\text{H}_8$  trends and their ERs at SGP and SGP-s (ONG sites). We

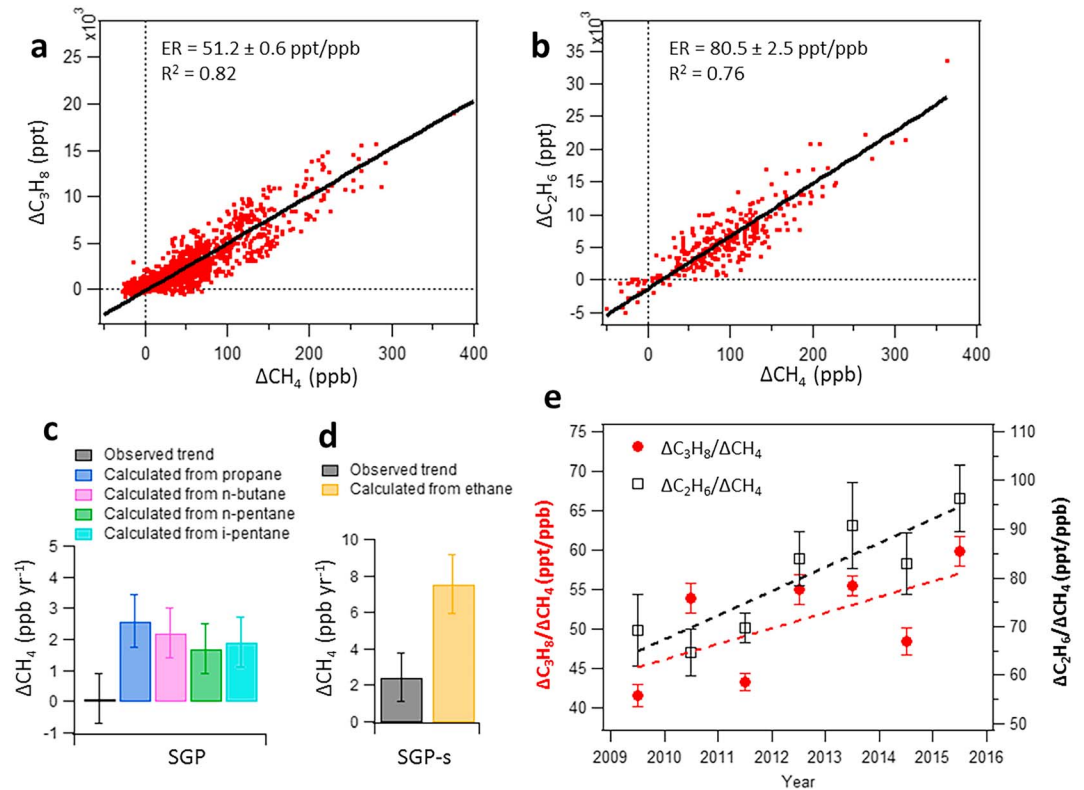


**Figure 3.** Enhancement ratios (ERs) and discrepancies between observed and calculated  $\Delta\text{CH}_4$  trends. (a) ER of  $\Delta\text{C}_3\text{H}_8/\Delta\text{CH}_4$  from aircraft measurements at SGP during 2009–2015. (b) ER of  $\Delta\text{C}_2\text{H}_6/\Delta\text{CH}_4$  from surface flask measurements at SGP-s during 2009–2015. (c and d) The observed and calculated  $\Delta\text{CH}_4$  trends using hydrocarbon data and their corresponding ERs (constant ERs from slopes in a and b). ERs in e are the same as in a and b but are derived on yearly basis. The dashed lines are linear fits to the ers; the trend for  $\Delta\text{C}_3\text{H}_8/\Delta\text{CH}_4$  is  $1.98 \pm 1.09 \text{ ppt} \cdot \text{ppb}^{-1} \cdot \text{year}^{-1}$  (red line) and  $4.94 \pm 1.13 \text{ ppt} \cdot \text{ppb}^{-1} \cdot \text{year}^{-1}$  for  $\Delta\text{C}_2\text{H}_6/\Delta\text{CH}_4$  (black line). All error bars shows  $1\sigma$  uncertainty.

find strong correlations between  $\Delta\text{C}_2\text{H}_6$  and  $\Delta\text{CH}_4$  at SGP-s, and  $\Delta\text{C}_3\text{H}_8$  and  $\Delta\text{CH}_4$  at SGP imply that most  $\Delta\text{CH}_4$  is from ONG emissions and influences from other sources (which do not contribute to  $\Delta\text{C}_3\text{H}_8$  and  $\Delta\text{C}_2\text{H}_6$ ) are not significant (also note that intercept is close to zero in Figures 3a and 3b). This is consistent with our footprint and inventory analysis.

The linear correlation can be written as

$$\Delta\text{HC} = \text{ER} \times \Delta\text{CH}_4 + \text{intercept} \quad (1)$$

Taking the time derivative of equation (1) gives

$$\frac{d(\Delta\text{HC})}{dt} = \text{ER} \times \frac{d(\Delta\text{CH}_4)}{dt} + \Delta\text{CH}_4 \times \frac{d(\text{ER})}{dt} \quad (2)$$

If ER is assumed constant over time (as done in previous studies (Franco et al., 2016, Hausmann et al., 2016, Helmig et al., 2016)), equation (2) becomes

$$\frac{d(\Delta\text{HC})}{dt} = \text{ER} \times \frac{d(\Delta\text{CH}_4)}{dt} \quad (3)$$

where  $\Delta\text{HC}$  represents the enhancement of any hydrocarbon compound that is well correlated with  $\Delta\text{CH}_4$ . Equation (3) has been used in other studies to derive  $\Delta\text{CH}_4$  trends from ONG emissions. However, when we apply equation (3), i.e., using the observed average  $\Delta\text{C}_3\text{H}_8/\Delta\text{CH}_4$  (from Figure 3a) and the observed  $\Delta\text{C}_3\text{H}_8$  trend to calculate  $\Delta\text{CH}_4$  trend ( $\frac{d(\Delta\text{CH}_4)}{dt}$ ) at SGP, we derive a  $\Delta\text{CH}_4$  trend that is much larger than the observed

trend (Figure 3c) because the missing term  $\Delta\text{CH}_4 \times \frac{d(\text{ER})}{dt}$  (due to simplification from equations (2) and (3)) has to be compensated by the derived  $\Delta\text{CH}_4$  trend. A similar overestimate in calculated  $\Delta\text{CH}_4$  trend is also found when using the average ER of  $\Delta\text{C}_2\text{H}_6/\Delta\text{CH}_4$  (Figure 3d, and for butane and pentanes; Figure 3c). These discrepancies are caused in part from ERs varying over time (see Figure 3e). As an example for SGP-s, the observed  $\Delta\text{C}_2\text{H}_6$  trend ( $\frac{d(\Delta\text{HFC})}{dt}$ ) equals  $610 \pm 130$  ppt/year, while  $\Delta\text{CH}_4 \times \frac{d(\text{ER})}{dt}$  equals  $494 \pm 113$  ppt/year for 2009–2015. Note that multiplying  $\frac{d(\text{ER})}{dt}$  with  $\Delta\text{CH}_4$  amplified the impact of the temporal variations of ER substantially. Thus, the simplified relationship in equation (3) is not valid. If equation (2) is used, the resulting  $\Delta\text{CH}_4$  trend is  $1.44 \pm 2.14$  ppb/year, which is much closer to the observed  $2.30 \pm 1.18$  ppb/year than using equation (3) (see Figure 3d). However, the large uncertainty in the  $1.44 \pm 2.14$  ppb/year trend makes the trend statistically insignificant ( $\sigma > 1.44$  ppb/year). This uncertainty mostly comes from the uncertainty of the observed  $\Delta\text{C}_2\text{H}_6$  trend and the uncertainty of the trend in ER which partially due to the imperfect correlation between  $\Delta\text{C}_2\text{H}_6$  and  $\Delta\text{CH}_4$ . Thus, equation (2) is not an optimized approach to estimate  $\Delta\text{CH}_4$  trend; instead, directly measurements provide better estimate.

The ONG production data reported by the U.S. Energy Information Agency (U.S. Energy Information Administration) demonstrate drastically different production trends for dry natural gas,  $\text{C}_2\text{H}_6$  and  $\text{C}_3\text{H}_8$  in the surrounding regions of SGP, with 36%, 99%, and 132% increases, respectively, in the last decade (Figure S1). The much higher relative increases in  $\text{C}_2\text{H}_6$  and  $\text{C}_3\text{H}_8$  than  $\text{CH}_4$  productions are qualitatively consistent with our findings about larger increases in  $\Delta\text{C}_2\text{H}_6$  and  $\Delta\text{C}_3\text{H}_8$  than  $\Delta\text{CH}_4$  (Figure 2) and the increasing trends in  $\Delta\text{C}_2\text{H}_6/\Delta\text{CH}_4$  and  $\Delta\text{C}_3\text{H}_8/\Delta\text{CH}_4$  (Figure 3e). These suggest that the total  $\text{CH}_4$ ,  $\text{C}_2\text{H}_6$ , and  $\text{C}_3\text{H}_8$  emissions from ONG activities may have increased at substantially different rates, reflecting the fundamental heterogeneity of ONG activities with respect to these chemicals, and possibly depending on economic shifts in the relative profitability of dry natural gas and other hydrocarbons. Previous short-term studies (Kort et al., 2016; Peischl et al., 2015) have reported large spatial differences in ERs from different ONG production fields, questioning the reliability of using a spatially universal ER to estimate ONG  $\text{CH}_4$  emissions for continental scale. Our study based on continuous long-term measurements further demonstrates how long-term trends in ER yield faulty ONG  $\text{CH}_4$  trend. The ER is neither spatially uniform nor constant in time. Assuming otherwise is not a reliable approach to infer ONG  $\text{CH}_4$  trends.

#### Acknowledgments

We thank Doug Guenther, Jack Higgs, Eric Moglia, Don Neff, and Sonja Wolter for their contributions to data collection; Andrew Crotwell for air sample analysis; Anna Karion for contributions to the aircraft sampling; Carolina Siso for conducting propane analysis; and Brad Hall for providing standard scales for propane and ethane. We thank NOAA Climate Program Office for supporting this study. Observations collected at the Southern Great Plains site were supported by the Office of Biological and Environmental Research of the US Department of Energy under contract DE-AC02-05CH11231 as part of the Atmospheric Radiation Measurement Program (ARM) and Terrestrial Ecosystem Science (TES) Program. Methane mole fraction data from aircraft measurements and surface flasks are provided by NOAA/OAR/ESRL GMD, publicly available at [https://www.esrl.noaa.gov/gmd/ccgg/obspack/data.php?Id=obspack\\_multi-species\\_1\\_ccggaircraftflask\\_v1.0\\_2018-02-08](https://www.esrl.noaa.gov/gmd/ccgg/obspack/data.php?Id=obspack_multi-species_1_ccggaircraftflask_v1.0_2018-02-08). [https://www.esrl.noaa.gov/gmd/ccgg/obspack/data.php?Id=obspack\\_multi-species\\_1\\_ccggsurfaceflask\\_v1.0\\_2018-02-08](https://www.esrl.noaa.gov/gmd/ccgg/obspack/data.php?Id=obspack_multi-species_1_ccggsurfaceflask_v1.0_2018-02-08). Aircraft and tall tower measured propane, butane, and pentanes data used in this research are available at <https://doi.org/10.15138/G3W92R>. Surface ethane and propane data (including KEY-s, THD-s, UTA-s, SGP-s, and MLO-s sites in this study) are publicly available at <https://www.esrl.noaa.gov/gmd/dv/data/>. NCEP Reanalysis data provided by the NOAA/OAR/ESRL PSD, Boulder, Colorado, USA, from their web site at <https://www.esrl.noaa.gov/psd/>.

## 5. Conclusions

Our analysis of direct mole fraction measurements suggests smaller increases in ONG  $\text{CH}_4$  emissions from the United States than those reported by several studies (Franco et al., 2016; Hausmann et al., 2016; Helmig et al., 2016; Turner et al., 2016). Although  $\text{C}_2\text{H}_6$  and  $\text{C}_3\text{H}_8$  are appropriate indicative tracers for ONG emissions, ONG  $\text{CH}_4$  trends cannot be accurately estimated from  $\text{C}_2\text{H}_6$  and  $\text{C}_3\text{H}_8$ . Thus, any conclusion of a large fossil  $\text{CH}_4$  increase in the past decade from studies that have used the constant ER assumption is unreliable. By comparing the  $\Delta\text{CH}_4$  trend from inflow and outflow sites of CONUS and considering the detectabilities of emission changes at these sites, we find no evidence to support a large increase in total U.S.  $\text{CH}_4$  emissions over the past decade, although we do find clear evidence of a modest increase in ONG  $\text{CH}_4$  emissions at three sites. By comparing the  $\Delta\text{CH}_4$  trend with trends in  $\Delta\text{C}_2\text{H}_6$  and  $\Delta\text{C}_3\text{H}_8$  at ONG sites, we also find that the increases in ONG  $\text{C}_2\text{H}_6$  and  $\text{C}_3\text{H}_8$  emissions are substantially larger on a relative basis than increases in ONG  $\text{CH}_4$  emissions.

## References

- Alvarez, R. A., Zavala-Araiza, D., Lyon, D. R., Allen, D. T., Barkley, A. R., Brandt, A. R., et al. (2018). Assessment of methane emissions from the U.S. oil and gas supply chain. *Science*, *361*, 186–188. <https://doi.org/10.1126/science.aar7204>
- Andrews, A. E., Kofler, J. D., Trudeau, M. E., Williams, J. C., Neff, D. H., Masarie, K. A., et al. (2014).  $\text{CO}_2$ , CO, and  $\text{CH}_4$  measurements from tall towers in the NOAA Earth System Research Laboratory's Global Greenhouse Gas Reference Network: Instrumentation, uncertainty analysis, and recommendations for future high-accuracy greenhouse gas monitoring efforts. *Atmospheric Measurement Techniques*, *7*(2), 647–687. <https://doi.org/10.5194/amt-7-647-2014>
- Ballantyne, A. P., Miller, J. B., & Tans, P. P. (2010). Apparent seasonal cycle in isotopic discrimination of carbon in the atmosphere and biosphere due to vapor pressure deficit. *Global Biogeochemical Cycles*, *24*, GB3018. <https://doi.org/10.1029/2009GB003623>
- Bousquet, P., Ciais, P., Miller, J. B., Dlugokencky, E. J., Hauglustaine, D. A., Prigent, C., et al. (2006). Contribution of anthropogenic and natural sources to atmospheric methane variability. *Nature*, *443*(7110), 439–443. <https://doi.org/10.1038/nature05132>
- Brandt, A. R., Heath, G. A., Kort, E. A., O'Sullivan, F., Petron, G., Jordaán, S. M., et al. (2014). Methane leaks from North American Natural Gas Systems. *Science*, *343*(6172), 733–735. <https://doi.org/10.1126/science.1247045>

- Bruhwyler, L. M., Basu, S., Bergamaschi, P., Bousquet, P., Dlugokencky, E., Houweling, S., et al. (2017). US CH<sub>4</sub> emissions from oil and gas production: Have recent large increases been detected? *Journal of Geophysical Research: Atmospheres*, *122*, 4070–4083. <https://doi.org/10.1002/2016JD026157>
- Butler, J. H., & Montzka, S. A. (2017). THE NOAA Annual Greenhouse Gas Index (AGGI). <https://www.esrl.noaa.gov/gmd/aggi/aggi.html>
- Dlugokencky, E. (2018). Trends in atmospheric methane. *NOAA/ESRL*, [https://www.esrl.noaa.gov/gmd/ccgg/trends\\_ch4/](https://www.esrl.noaa.gov/gmd/ccgg/trends_ch4/)
- Dlugokencky, E. J., Bruhwiler, L., White, J. W. C., Emmons, L. K., Novelli, P. C., Montzka, S. A., et al. (2009). Observational constraints on recent increases in the atmospheric CH<sub>4</sub> burden. *Geophysical Research Letters*, *36*, L18803. <https://doi.org/10.1029/2009GL039780>
- Dlugokencky, E. J., Houweling, S., Bruhwiler, L., Masarie, K. A., Lang, P. M., Miller, J. B., & Tans, P. P. (2003). Atmospheric methane levels off: Temporary pause or a new steady-state? *Geophysical Research Letters*, *30*(19), 1992. <https://doi.org/10.1029/2003GL018126>
- Dlugokencky, E. J., Lang, P. M., Crotwell, A. M., Masarie, K. A., Crotwell, M. J., & Tans, P. P. (2015). Atmospheric methane dry air mole fractions from the NOAA ESRL Carbon Cycle Cooperative Global Air Sampling Network. Data Path: [ftp://aftp.cmdl.noaa.gov/data/trace\\_gases/ch4/flask/surface/](ftp://aftp.cmdl.noaa.gov/data/trace_gases/ch4/flask/surface/)
- Franco, B., Mahieu, E., Emmons, L. K., Tzompa-Sosa, Z. A., Fischer, E. V., Sudo, K., et al. (2016). Evaluating ethane and methane emissions associated with the development of oil and natural gas extraction in North America. *Environmental Research Letters*, *11*(4), 11. <https://doi.org/10.1088/1748-9326/11/4/044010>
- Goldstein, A. H., Wofsy, S. C., & Spivakovsky, C. M. (1995). Seasonal-variations of nonmethane hydrocarbons in rural New England—Constraints on OH concentrations in northern midlatitudes. *Journal of Geophysical Research*, *100*(D10), 21,023–21,033. <https://doi.org/10.1029/95JD02034>
- Hausmann, P., Sussmann, R., & Smale, D. (2016). Contribution of oil and natural gas production to renewed increase in atmospheric methane (2007–2014): Top-down estimate from ethane and methane column observations. *Atmospheric Chemistry and Physics*, *16*(5), 3227–3244. <https://doi.org/10.5194/acp-16-3227-2016>
- Helmig, D., Rossabi, S., Hueber, J., Tans, P., Montzka, S. A., Masarie, K., et al. (2016). Reversal of global atmospheric ethane and propane trends largely due to US oil and natural gas production. *Nature Geoscience*, *9*(7), 490–495. <https://doi.org/10.1038/ngeo2721>
- Helmig, D., Thompson, C. R., Evans, J., Boylan, P., Hueber, J., & Park, J. H. (2014). Highly elevated atmospheric levels of volatile organic compounds in the Uintah Basin, Utah. *Environmental Science & Technology*, *48*(9), 4707–4715. <https://doi.org/10.1021/es405046r>
- Hristov, A. N., Harper, M., Meinen, R., Day, R., Lopes, J., Ott, T., et al. (2017). Discrepancies and uncertainties in bottom-up gridded inventories of livestock methane emissions for the contiguous United States. *Environmental Science & Technology*, *51*(23), 13,668–13,677. <https://doi.org/10.1021/acs.est.7b03332>
- Kort, E. A., Smith, M. L., Murray, L. T., Gvakharia, A., Brandt, A. R., Peischl, J., et al. (2016). Fugitive emissions from the Bakken shale illustrate role of shale production in global ethane shift. *Geophysical Research Letters*, *43*, 4617–4623. <https://doi.org/10.1002/2016GL068703>
- Lehner, B., & Doll, P. (2004). Development and validation of a global database of lakes, reservoirs and wetlands. *Journal of Hydrology*, *296*(1–4), 1–22. <https://doi.org/10.1016/j.jhydrol.2004.03.028>
- Maasakkers, J. D., Jacob, D. J., Sulprizio, M. P., Turner, A. J., Weitz, M., Wirth, T., et al. (2016). Gridded National Inventory of US Methane Emissions. *Environmental Science & Technology*, *50*(23), 13,123–13,133. <https://doi.org/10.1021/acs.est.6b02878>
- Miller, J. B., Lehman, S. J., Montzka, S. A., Sweeney, C., Miller, B. R., Karion, A., et al. (2012). Linking emissions of fossil fuel CO<sub>2</sub> and other anthropogenic trace gases using atmospheric (CO<sub>2</sub>)-C-14. *Journal of Geophysical Research*, *117*, D08302. <https://doi.org/10.1029/2011JD017048>
- Miller, S. M., Wofsy, S. C., Michalak, A. M., Kort, E. A., Andrews, A. E., Biraud, S. C., et al. (2013). Anthropogenic emissions of methane in the United States. *Proceedings of the National Academy of Sciences of the United States of America*, *110*(50), 20,018–20,022. <https://doi.org/10.1073/pnas.1314392110>
- Nisbet, E. G., Dlugokencky, E. J., Manning, M. R., Lowry, D., Fisher, R. E., France, J. L., et al. (2016). Rising atmospheric methane: 2007–2014 growth and isotopic shift. *Global Biogeochemical Cycles*, *30*, 1356–1370. <https://doi.org/10.1002/2016GB005406>
- Peischl, J., Karion, A., Sweeney, C., Kort, E. A., Smith, M. L., Brandt, A. R., et al. (2016). Quantifying atmospheric methane emissions from oil and natural gas production in the Bakken shale region of North Dakota. *Journal of Geophysical Research: Atmospheres*, *121*, 6101–6111. <https://doi.org/10.1002/2015JD024631>
- Peischl, J., Ryerson, T. B., Aikin, K. C., de Gouw, J. A., Gilman, J. B., Holloway, J. S., et al. (2015). Quantifying atmospheric methane emissions from the Haynesville, Fayetteville, and northeastern Marcellus shale gas production regions. *Journal of Geophysical Research: Atmospheres*, *120*, 2119–2139. <https://doi.org/10.1002/2014JD022697>
- Rudolph, J. (1995). The tropospheric distribution and budget of ethane. *Journal of Geophysical Research*, *100*(D6), 11,369–11,381. <https://doi.org/10.1029/95JD00693>
- Saunio, M., Bousquet, P., Poulter, B., Peregón, A., Ciais, P., Canadell, J. G., et al. (2016). The global methane budget 2000–2012. *Earth System Science Data*, *8*(2), 697–751. <https://doi.org/10.5194/essd-8-697-2016>
- Schaefer, H., Fletcher, S. E. M., Veidt, C., Lassef, K. R., Brailsford, G. W., Bromley, T. M., et al. (2016). A 21st-century shift from fossil-fuel to biogenic methane emissions indicated by (CH<sub>4</sub>)-C-13. *Science*, *352*(6281), 80–84. <https://doi.org/10.1126/science.aad2705>
- Schwietzke, S., Sherwood, O. A., Ruhwiler, L., Miller, J. B., Etiope, G., Dlugokencky, E. J., et al. (2016). Upward revision of global fossil fuel methane emissions based on isotope database. *Nature*, *538*(7623), 88–91. <https://doi.org/10.1038/nature19797>
- Smith, M. L., Kort, E. A., Karion, A., Sweeney, C., Herndon, S. C., & Yacovitch, T. I. (2015). Airborne ethane observations in the Barnett Shale: Quantification of ethane flux and attribution of methane emissions. *Environmental Science & Technology*, *49*(13), 8158–8166. <https://doi.org/10.1021/acs.est.5b00219>
- Sweeney, C., Karion, A., Wolter, S., Newberger, T., Guenther, D., Higgs, J. A., et al. (2015). Seasonal climatology of CO<sub>2</sub> across North America from aircraft measurements in the NOAA/ESRL Global Greenhouse Gas Reference Network. *Journal of Geophysical Research: Atmospheres*, *120*, 5155–5190. <https://doi.org/10.1002/2014JD022591>
- Turner, A. J., Jacob, D. J., Benmergui, J., Wofsy, S. C., Maasakkers, J. D., Butz, A., et al. (2016). A large increase in US methane emissions over the past decade inferred from satellite data and surface observations. *Geophysical Research Letters*, *43*, 2218–2224. <https://doi.org/10.1002/2016GL067987>
- United States Energy Information Administration (2016). Hydraulically fractured wells provide two-thirds of U.S. natural gas production. <https://www.eia.gov/todayinenergy/detail.php?id=26112>
- United States Environmental Protection Agency (2017). Inventory of U.S. greenhouse gas emissions and sink. 2. Trends in greenhouse gas emissions. [https://www.epa.gov/sites/production/files/2017-02/documents/2017\\_chapter\\_2\\_trends\\_in\\_greenhouse\\_gas\\_emissions.pdf](https://www.epa.gov/sites/production/files/2017-02/documents/2017_chapter_2_trends_in_greenhouse_gas_emissions.pdf)
- Wolf, J., Asrar, G. R., & West, T. O. (2017). Revised methane emissions factors and spatially distributed annual carbon fluxes for global livestock. *Carbon Balance and Management*, *12*(1), 16. <https://doi.org/10.1186/s13021-017-0084-y>



## References From the Supporting Information

- Biraud, S. C., Torn, M. S., Smith, J. R., Sweeney, C., Riley, W. J., & Tans, P. P. (2013). A multi-year record of airborne CO<sub>2</sub> observations in the US Southern Great Plains. *Atmospheric Measurement Techniques*, 6(3), 751–763. <https://doi.org/10.5194/amt-6-751-2013>
- Diaconis, P., & Efron, B. (1983). Computer-intensive methods in statistics. *Scientific American*, 248(5), 116–130.
- Dlugokencky, E. J., Myers, R. C., Lang, P. M., Masarie, K. A., Crotwell, A. M., Thoning, K. W., et al. (2005). Conversion of NOAA atmospheric dry air CH<sub>4</sub> mole fractions to a gravimetrically prepared standard scale. *Journal of Geophysical Research*, 110, D18306. <https://doi.org/10.1029/2005JD006035>
- Kalnay, E., Kanamitsu, M., Kistler, R., Collins, W., Deaven, D., Gandin, L., et al. (1996). The NCEP/NCAR 40-year reanalysis project. *Bulletin of The American Meteorological Society*, 77(3), 437–471.
- Lin, J. C., Gerbig, C., Wofsy, S. C., Andrews, A. E., Daube, B. C., Davis, K. J., & Grainger, C. A. (2003). A near-field tool for simulating the upstream influence of atmospheric observations: The Stochastic Time-Inverted Lagrangian Transport (STILT) model. *Journal of Geophysical Research*, 108(D16), 4493. <https://doi.org/10.1029/2002JD003161>
- Miller, S. M., Commene, R., Melton, J. R., Andrews, A. E., Benmergui, J., Dlugokencky, E. J., et al. (2016). Evaluation of wetland methane emissions across North America using atmospheric data and inverse modeling. *Biogeosciences*, 13(4), 1329–1339. <https://doi.org/10.5194/bg-13-1329-2016>
- Montzka, S. A., Calvert, P., Hall, B. D., Elkins, J. W., Conway, T. J., Tans, P. P., & Sweeney, C. (2007). On the global distribution, seasonality, and budget of atmospheric carbonyl sulfide (COS) and some similarities to CO<sub>2</sub>. *Journal of Geophysical Research*, 112, D09302. <https://doi.org/10.1029/2006JD007665>
- Montzka, S. A., Myers, R. C., Butler, J. H., Elkins, J. W., & Cummings, S. O. (1993). Global tropospheric distribution and calibration scale of HCFC-22. *Geophysical Research Letters*, 20(8), 703–706. <https://doi.org/10.1029/93GL00753>
- Nehrkorn, T., Eluszkiewicz, J., Wofsy, S. C., Lin, J. C., Gerbig, C., Longo, M., & Freitas, S. (2010). Coupled weather research and forecasting-stochastic time-inverted Lagrangian transport (WRF-STILT) model. *Meteorology and Atmospheric Physics*, 107(1-2), 51–64. <https://doi.org/10.1007/s00703-010-0068-x>
- Pollmann, J., Helmig, D., Hueber, J., Plass-Dulmer, C. A., & Tans, P. (2008). Sampling, storage, and analysis of C-2-C-7 non-methane hydrocarbons from the US National Oceanic and Atmospheric Administration Cooperative Air Sampling Network glass flasks. *Journal of Chromatography. A*, 1188(2), 75–87. <https://doi.org/10.1016/j.chroma.2008.02.059>
- Pollmann, J., Helmig, D., Hueber, J., Tanner, D., & Tans, P. P. (2006). Evaluation of solid adsorbent materials for cryogen-free trapping—Gas chromatographic analysis of atmospheric C<sub>2</sub>-C<sub>6</sub> non-methane hydrocarbons. *Journal of Chromatography. A*, 1134(1-2), 1–15. <https://doi.org/10.1016/j.chroma.2006.08.050>
- Thoning, K. W., Tans, P. P., & Komhyr, W. D. (1989). Atmospheric carbon-dioxide at Mauna Loa Observatory.2. Analysis of the NOAA GMCC data, 1974-1985. *Journal of Geophysical Research*, 94(D6), 8549–8565. <https://doi.org/10.1029/JD094iD06p08549>
- United States Energy Information Administration Natural Gas Production (2018). <https://www.eia.gov/naturalgas/data.php#production>.
- Werner, C., Davis, K., Bakwin, P., Yi, C. X., Hurst, D., & Lock, L. (2003). Regional-scale measurements of CH<sub>4</sub> exchange from a tall tower over a mixed temperate/boreal lowland and wetland forest. *Global Change Biology*, 9(9), 1251–1261. <https://doi.org/10.1046/j.1365-2486.2003.00670.x>